Spectral hole-burning in uranium-doped tungstates

Keith Holliday and Neil B Manson

Laser Physics Centre, Research School of Physical Sciences, The Australian National University, GPO Box 4, Canberra, ACT 2601, Australia

Abstract. This paper describes the first observation of persistent spectral hole-burning in actinide-ion-doped crystals. Spectral hole-burning in three zero-phonon lines at 652.1 nm, 658.4 nm and 659.1 nm in $SrWO_4$:U and one zero-phonon line at 654.4 nm in $BaWO_4$:U is reported. The holes display quadratic Zeeman shifts. Also when the field is along the $\langle 110 \rangle$ direction the holes are split into two indicating the presence of two crystallographically equivalent sites of C_2 symmetry. This is explained in terms of U^{6+} ions substituting for W^{6+} but having two equilibrium positions displaced in alternate directions along the c axis from the substitutional site. As well as narrow holes there are broad anti-holes, resulting in an unchanged integrated absorption showing that the hole-burning is photophysical. The mechanism is attributed to the reorientation of the U^{6+} between the two sites.

1. Introduction

Persistent optical holes have been burnt in the zero-phonon spectral lines of ionic solids doped with transition-metal ions (Jessop *et al* 1980, Macfarlane and Vial 1986, Macfarlane and Lenth 1986) and lanthanide ions (Macfarlane and Shelby 1987). The mechanism for such hole-burning can be through population changes in the electron or nuclear spin levels, through photochemical changes involving the valence of the impurity ion or physical changes involving the movement of an ion or ions within the crystal host lattice or glass (Macfarlane and Shelby 1987).

The absorption and emission of uranium-doped tungstates and molybdates have been reported by Morozov *et al* (1972). 't Lam and Blasse (1980) have also measured the excitation spectrum and studied the radiative decay and quenching as a function of temperature. In these studies it was established that there was little difference between the tungstates and the equivalent molybdates such that the present work is restricted to one: the tungstates. More significant differences occur when the anion is changed from calcium to strontium or barium. In the case of the calcium crystals all the spectral bands were structureless whereas with strontium and barium the spectra displayed several sharp lines. This results in the strontium and barium materials being more amenable to spectroscopic study and are found to be the only ones exhibiting spectral hole-burning. In the earlier work (Morozov *et al* 1972, 't Lam and Blasse 1980) it was taken that uranium ions substituted directly for tungsten ions, but higher-resolution measurements using spectral holes enable us to show that this is inaccurate. The site symmetry can be determined reliably and reasonable models proposed for the geometry of the centre. The hole-burning mechanism can also be established.
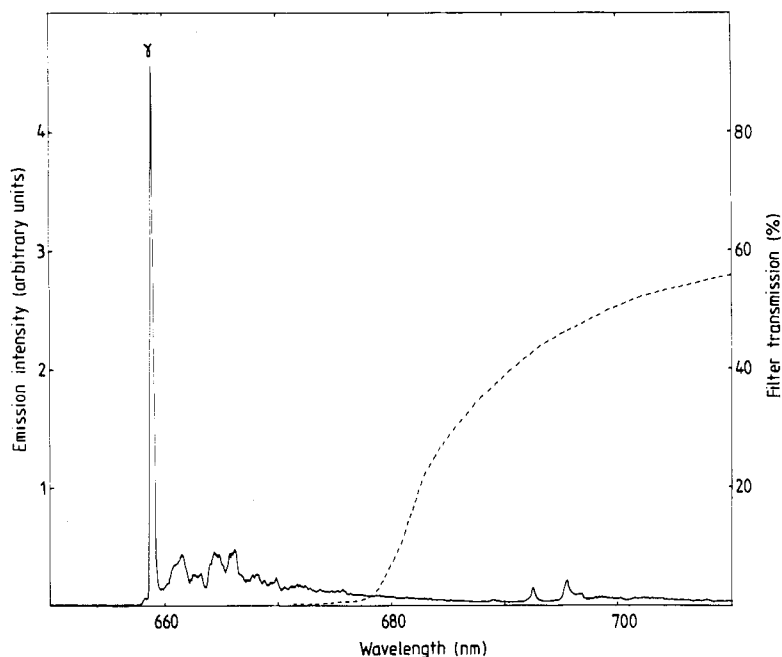
Figure 1. The emission spectrum of $SrWO_4$:U at 10 K measured in σ-polarisation. The broken curve indicates the transmission of the filter used for recording excitation spectra.

2. Experimental details

Crystals were pulled from the melt in an argon atmosphere using the Czochralski method. Crystals of the order of $2 \times 4 \times 3$ mm³ were cut from the boule and oriented using Laue back-reflection x-ray diffraction. Microprobe techniques determined the uranium concentrations to be 200 ppm for the strontium tungstate samples used in all experiments except the low-resolution hole-burning. The sample used for this latter technique had a uranium concentration of 500 ppm. The barium tungstate crystals had an estimated concentration of 100 ppm of uranium.

The initial spectroscopy was performed using a Molectron DLII tunable dye laser pumped by a Molectron pulsed nitrogen laser. The crystal was mounted in a flow tube and cooled to 10 K. The temperature could be varied by varying the helium flow rate and monitored by measuring the voltage drop across a carbon resistor (270 Ω at room temperature) mounted next to the crystal. The emission was detected by a photomultiplier after being dispersed by a monochromator. As only one centre is present in this region of the spectrum, all or any part of the emission could be detected in order to determine the excitation spectrum. Likewise, the fluorescence spectrum could be determined by pumping at any wavelength within the excitation spectrum.

For hole-burning experiments the emission passing through a Corion LG-697 long-wavelength pass filter was detected perpendicular to the laser beam. The filter eliminates the detection of scattered laser light but allows the detection of emission in the low-energy part of the band (figure 1).

High-resolution hole-burning experiments were performed using a Coherent 699-21 ring dye laser with a linewidth of 1 MHz pumped by a Spectra-Physics 171 argon-ion laser. The crystals were in helium exchange gas and mounted on a rod that allowed for rotation of the sample in the coils of a superconducting magnet.
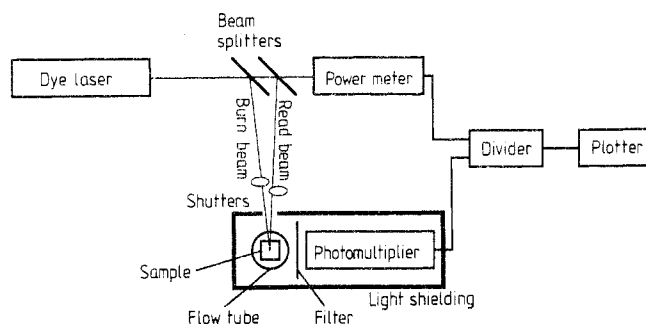
Figure 2. The experimental apparatus for spectral hole-burning.

Low-resolution hole-burning experiments were performed using a Spectra-Physics 375 dye laser with a line width of 30 GHz pumped by a Spectra-Physics 171 argon-ion laser. The crystal was again mounted in a flow tube and cooled to 10 K. To give the required accuracy in the measurement of the line profile the beam was split into three components (figure 2). 90% of the beam power was directed onto the crystal during hole-burning and was blocked whilst recording the line profile. 6% of the beam power was directed onto the same part of the crystal and was used as the excitation source whilst recording data. The remaining 4% was used to monitor power fluctuations. This signal was divided into the photomultiplier signal to provide a normalised emission signal. The total power output from the dye laser was 200 mW.

Absorption measurements were made on a single-beam instrument with a tungsten light source.

3. Results and discussion

3.1. Absorption, emission and excitation

Three excited electronic levels have been located, consistent with earlier work (Morozov *et al* 1972). In strontium tungstate they give rise to zero-phonon lines in absorption at 652.1 nm (α), 658.4 nm (β) and 659.1 nm (γ), and in barium tungstate at 647.6 nm (α), 654.4 nm (β) and 656.3 nm (γ). In the latter material the γ-absorption was weak and the presence of this level could only be confirmed by fluorescence line-narrowing techniques. The α- and γ-lines are σ ($E \perp c$) polarised and β-line is π ($E \parallel c$) polarised. For the 200 ppm uranium-doped strontium tungstate crystal the excitation spectrum is shown in figure 3 and it is found that due to scattered light the lines were not so markedly polarised as in absorption. The associated emission has been shown in figure 1. In the more heavily uranium-doped strontium tungstate samples the inhomogenous broadening was larger for all three zero-phonon lines, causing the β- and γ-lines to overlap.

3.2. Hole-burning

In strontium tungstate, holes could be burnt in all three zero-phonon lines. At 4.2 K, holes burnt in the lowest-energy level (γ) were limited in width by laser jitter and it can be concluded that the homogeneous linewidth of the transition is less than 1 MHz. Holes burnt in the β-line had a width of 20 MHz. Interaction may take place with any centre
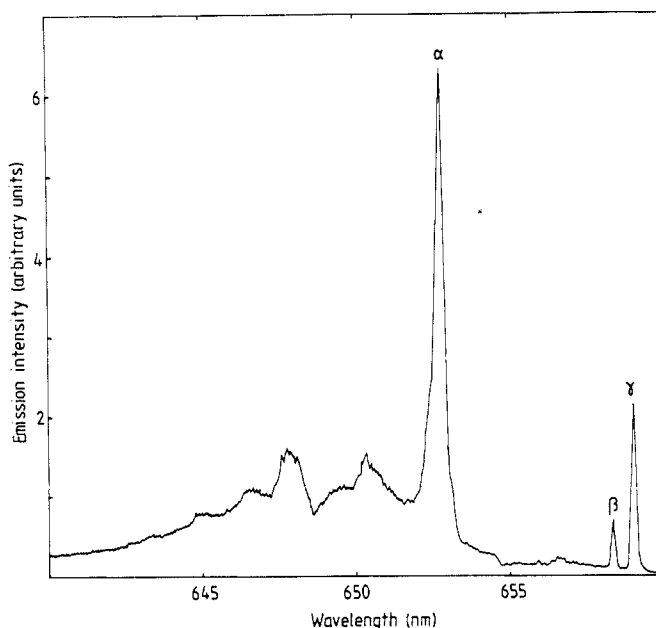
Figure 3. The excitation spectrum of $SrWO_4$: U at 10 K measured in σ-polarisation. The β zero-phonon transition is π-polarised but is seen here due to scattering of light within the crystal.

whose transition energy is within one homogeneous linewidth in both the burning and reading process and hence the homogeneous linewidth is half the holewidth, that is 10 MHz. This homogeneous linewidth will be established through direct phonon emission to the γ-level.

Hole-burning in the α-line could only be detected in the strongly doped sample where the inhomogeneous linewidth was found to be 1300 GHz. The holes had a width of 400 GHz and hence the homogeneous linewidth is 200 GHz, again determined by direct phonon emission to lower levels. It is not surprising that the weakly doped sample did not exhibit hole-burning as its inhomogeneous linewidth was only 500 GHz.

Figure 4 shows the line profiles of the β- and γ-lines in the highly doped samples after a hole has been burnt into the centre of the β-line with the low-resolution dye laser. As a result a hole has also been burnt in the centre of the γ-line with similar depth and width indicating that the strain which causes the inhomogeneous broadening does not alter the separation between energy levels. Due to the overlapping of the inhomogeneous lines, a hole is also burnt directly in the high-energy tail of the γ-line coincident with the central hole in the β-line. The corresponding hole in the high-energy tail of the β-line, although weak, can be observed.

Due to the weakness of the γ-absorption, hole-burning in the barium tungstate crystals was restricted to the β zero-phonon line. These holes were laser linewidth limited as the close proximity of the β- and γ-lines (5 cm^{-1}) causes little hole broadening due to the direct phonon emission from the β-level to the γ-level.

3.3. Zeeman effect and site symmetry

Holes burnt with the high-resolution dye laser in the β- and γ-lines were found to be displaced quadratically in a magnetic field. When the field is applied perpendicular to
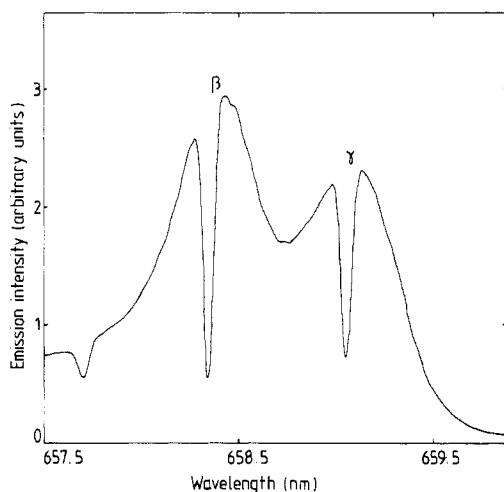
Figure 4. Optical hole-burning in a concentrated $SrWO_4$: U crystal at 10 K measured in the π-polarisation. The α zero-phonon transition is σ-polarised but is seen here due to scattering of light within the crystal. The hole has been burned at 658.3 nm and causes burning in the β-line at this frequency and a side hole in the γ-line at 659.0 nm. It also burns a hole in the component of the α-line at 658.3 nm and gives a side hole in β at shorter wavelength.

the c axis of the crystal as well as being displaced, the hole splits (figure 5). Upon rotating the crystal about the c axis the hole splitting was found to vary and for strontium tungstate is shown in figure 6. The maximum splitting occurs when the field is $30° \pm 5°$ from a $\langle 100 \rangle$ direction and after successive 90° rotations whereas the holes merge at 45° to maxima. When the field was out of the a–b plane there was a splitting into two lines. However when the field was applied along the c axis a shift but no splitting was observed. Table 1 summarises the size of these hole shifts for the β and γ-lines in strontium tungstate and for the β-line in barium tungstate.

All Zeeman shifts are quadratic, indicating that the symmetry is sufficiently low that all degeneracy has been lifted. In addition, the splitting indicates that there are two crystallographically equivalent but magnetically inequivalent centres within the solid. $SrWO_4$ has a scheelite lattice structure (No 88, C_{4h}^6 in Schönflies notation) and the uranium ion may occupy a position of S_4, C_2, S_2 or C_1 symmetry (*International Tables for X-ray Crystallography* 1969). The uranium ions presumably substitute for the tungsten ions which are in sites of S_4 symmetry but cannot remain precisely at the substitutional site as the S_4 group still has a twofold-degenerate irreducible representation. The splitting pattern indicates that the two sets of centres are oriented perpendicular to each other and the most probable explanation is for the uranium ion to be displaced up or down the c axis from the central site (figure 7). Clearly some relaxation of the oxygen may also be involved. The displacement lowers the symmetry from S_4 to C_2 and there are two such centres with their principal axes (local z axes) aligned with the S_4 principal axis but with their local x and y axes orthogonal. This can be seen by considering the nearest-neighbour oxygens. As the oxygen ions are arranged approximately tetrahedrally in the lattice with the displaced uranium ion lying closer to one pair of oxygen ions, there would then exist two perpendicularly oriented sets of centres. Furthermore, the axis joining the pair of oxygen ions in the tungstate lattice lies at an angle of 29° and $-61°$ to the $\langle 100 \rangle$ direction. These angles coincide, within the limits of experimental uncertainty, with the magnetic field angle required to give a maximum splitting (the angles are the same but the signs have not been determined). Thus it would seem clear
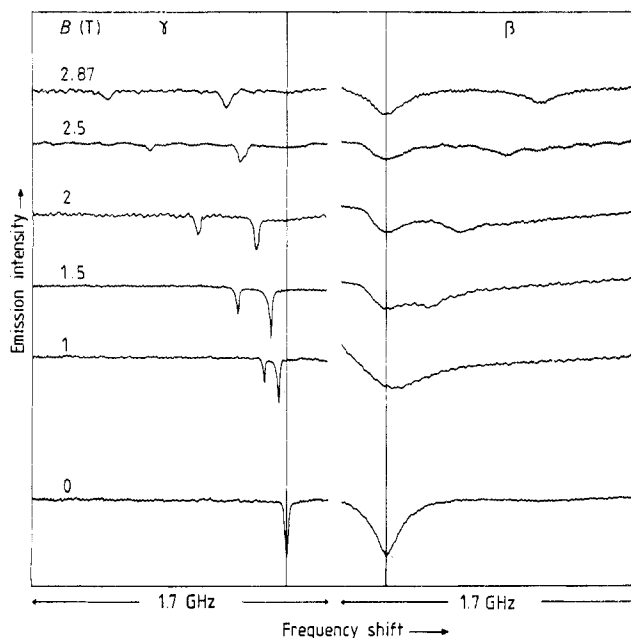
Figure 5. Quadratic Zeeman shifts of spectral holes in the γ and β zero-phonon lines in $SrWO_4$: U. The magnetic field is perpendicular to the c axis of the crystal at 30° to $\langle 100 \rangle$—the direction of maximum splitting.

that a magnetic field aligned directly along (or perpendicular to) one of the oxygen pairs gives the maximum quadratic Zeeman displacement. This is defined as the local x axis. When the field is along the x axis of one C_2 centre it will be along the local y axis of the other C_2 centre and gives a significantly smaller shift, if any. When the field is applied along the c axis of the crystal it is along the local z axis of both centres. They are magnetically equivalent and hole shifts will be equal, with no resultant splitting.

S_2 and C_1 are also possible site symmetries for the uranium centre. The sites of S_2 symmetry may be ruled out as the group has inversion symmetry and no electric dipole transitions are allowed. However, Morozov *et al* (1972) have shown that the zero-phonon transitions are electric dipole in nature. If the uranium were substituted into C_1 sites, our axial and transverse magnetic field results could be explained. However for a general field direction, at an angle other than 0° or 90° to the c axis, there would be four

Table 1. Quadratic Zeeman shifts.

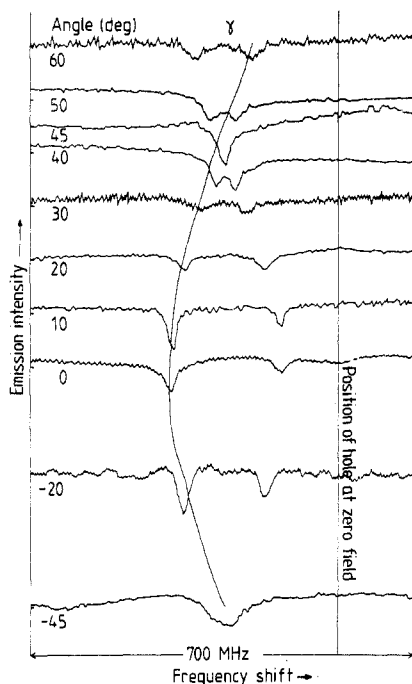| Material	Zero-phonon line	Energy ($\gamma = 0$) (cm^{-1})	$H \parallel x_{local}$	$H \parallel y_{local}$	$H \parallel z_{local}$
			H (MHz T^{-2})		
$SrWO_4$:U	α	161	—	—	—
	β	16	110	0	−20
	γ	0	−130	−40	−20
$BaWO_4$:U	α	164	—	—	—
	β	6	400	0	−10
	γ	0	—	—	—

Figure 6. The position and splitting of hole in the γ-line in $SrWO_4$:U as affected by the magnetic field direction in the (001) plane. The hole has been burned at zero field at the frequency indicated. An external magnetic field of 1 T is then applied and the hole-burning spectra measured. 0° corresponds to the position of maximum splitting (at 30° to $\langle 100 \rangle$).
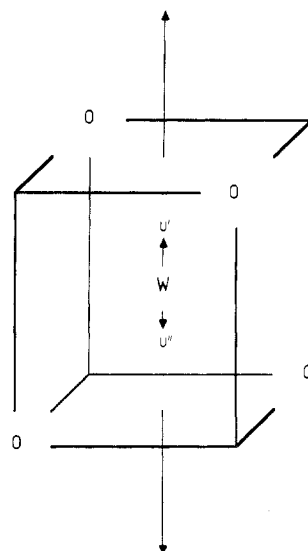
Figure 7. The S_4 substitutional site in the scheelite structure. W represents the site in the perfect crystal, whereas if the W^{6+} is replaced by U^{6+} then the equilibrium position can be at U' or U'', both with C_2 symmetry.

inequivalent sites. This would cause the hole to split into four components, which was not observed. The elimination of S_2 and C_1 site symmetries confirms our conclusion that the uranium ion is at a site of C_2 symmetry.

There are only two irreducible representations, Γ_1 or Γ_2, in the C_2 group. The ground state of hexavalent uranium has a closed electron shell and hence will transform as the symmetric Γ_1 irreducible representation. The α- and γ-lines are completely polarised perpendicular to the c axis (σ-spectrum) in absorption and therefore must be associated with excited Γ_2 state. The β-line is polarised along the c axis in absorption (π-spectrum) and will be associated with a Γ_1 state.

The quadratic Zeeman shifts occur when there is an interaction between adjacent levels and the necessary off-diagonal Zeeman matrix elements are only non-zero if the cross product of the states and magnetic field irreducible representation contains the symmetry representation. In C_2 symmetry the two possibilities are

$$\Gamma_1 \times \Gamma_1 \times \Gamma_1 = \Gamma_1 \qquad \Gamma_1 \times \Gamma_2 \times \Gamma_2 = \Gamma_1$$

A magnetic field along the crystal c axis and hence the local z axis transforms as a Γ_1 irreducible representation and can therefore cause levels with the irreducible representations to interact. A magnetic field perpendicular to the c axis transforms as a Γ_2 irreducible representation and can cause levels with unlike irreducible representations
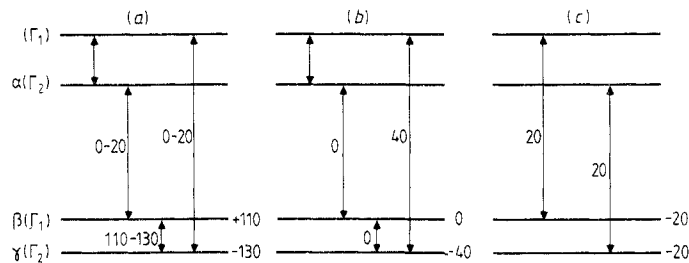
Figure 8. A summary of quadratic Zeeman interactions in $SrWO_4$: U in units of MHz T^{-2}. The experimental shifts of the β- and γ-lines are given adjacent to the levels. The strengths of the various interactions are given beside the arrows although when more than one interaction with a given level is involved the magnitude of the separate interactions cannot be uniquely determined. The magnetic field is along the local (a) x axis (Γ_2), (b) y axis (Γ_2) and (c) z axis (Γ_1).

to interact.

The α and γ zero-phonon lines associated with Γ_2 states should therefore interact when a magnetic field is applied along the c axis. No movement of the α-level can be measured as the level is too broad but the proposed interaction is consistent with the observation that holes burned in the γ-line shifted to lower energy with $H \parallel z$. The same field, however, also causes holes in the β-line in both $BaWO_4$: U and $SrWO_4$: U to be displaced to lower energy. The β-line is associated with a Γ_1 level and therefore there must be a further Γ_1 level at higher energy. 't Lam and Blasse (1979) have suggested that there is a fourth electronic level 927 cm^{-1} above the β-level in $SrWO_4$: U. It is not clear how this was distinguished from the vibronic sideband of the α zero-phonon line, but is too high in energy to account for the observed Zeeman shifts of the β-level. The more likely location of the relevant Γ_1 level is adjacent to the α-level lying just within the vibronic band.

The perpendicular field will give interactions between unlike symmetry states both adjacent (16 cm^{-1} in $SrWO_4$) and more distant (160 cm^{-1}) and the size of the individual interactions cannot be uniquely deduced from present measurements. Clearly however the interaction between adjacent levels is likely to be dominant. This is certainly true for one direction, defined as local x axis, where there is a large repulsion (≈ 120 MHz T^{-2} in $SrWO_4$) of β- and γ-levels. For the orthogonal centre where the field is along the local y axis, the shifts are zero for both $SrWO_4$ and $BaWO_4$ and this is taken as an indication that the interaction itself is small rather than the two interactions are cancelling. For $SrWO_4$ the size of these interactions are summarised in figure 8.

For two levels separated by an energy, ε, interacting through an off-diagonal Zeeman interaction ($g_{eff}\mu_B H$) the repulsion of levels is given by

$$\Delta E = g_{eff}^2 \mu_B^2 H^2 / \varepsilon.$$

Therefore the strengths of the above interactions can be characterised by the size of the effective g-value. For adjacent levels this gives for $H \parallel x$ values of $g_{eff} = 0.38$ and $g_{eff} = 1.60$ for $SrWO_4$ and $BaWO_4$ respectively. Interaction between levels 160 cm^{-1} apart give values of $g_{eff} = 1.5$ and 2.0 respectively. The magnitudes are, in general, larger than the g-values obtained for degenerate first excited states of U^{6+} in uranyl (Denning *et al* 1976) and in an octahedral environment (Runciman *et al* 1986) but indicate that with the large spin–orbit parameter there is a significant orbital contribution in determination of

the Zeeman interaction.

Although there has been significant progress towards understanding the electron configurations involved in the excited states of hexavalent uranium in uranyl ions (Denning *et al* 1979), in molecules such as UF_6 (Hay 1983) and in complexes such as UO_5F (Runciman *et al* 1986), so far there has been no work dealing with the tetrahedral unit. Analogous to the linear and octahedral environments it is expected that the excited states will be formed from the transfer of an electron from a nearest-neighbour oxygen to an f-electron orbit on the uranium. This results in a large number of possible electron–hole states and assumptions concerning the relative energies of the a_1, t_1 and t_2 f-electron orbits and the σ and π ligand orbitals are desirable. Consideration must first be given to the magnitude of the distortions lowering the symmetry from T_d to S_4 and C_2. In this regard the near degeneracy of the β- and γ-levels (16 cm^{-1} separation in $SrWO_4$ and 6 cm^{-1} in $BaWO_4$) is taken to be significant. The Zeeman perturbation that has the largest effect on their separation is that with the field at right angles to the crystal *c* axis implying an approximate higher-symmetry system with a principal axis in the *a–b* plane. The uranium ion could, for example, lie between two oxygen ions with the other two oxygen ions being at a somewhat larger distance giving a perturbed linear molecule. This is reasonably consistent with the Zeeman data particularly as it was shown that it was a field along the oxygen–oxygen axis, the axis of the perturbed linear molecule, that gave the maximum Zeeman effect. However, none of the other spectroscopic characteristics of the system, such as emission wavelength, *g*-values or features at many multiples of the symmetric mode frequency ($\nu = 730$ cm^{-1}), are in any way like that of a uranyl ion. Thus the origin of the approximate symmetry in the *a–b* plane is not clear and the exact geometry of the centre must therefore still be in some doubt. Detailed modelling of the excited-state electron configurations is not warranted at this stage.

3.4. The hole-burning mechanism

For determination of the hole-burning mechanisms there are several additional experimental observations that have to be considered.

(i) Holes burnt in the β- and γ-lines using the low-resolution dye laser in the dilute sample were found to be filled by irradiation at the wavelength of the α zero-phonon line using the same laser power for a similar period of time as was used to burn the hole.

(ii) In the concentrated sample, equivalent experiments revealed that the overall distributions of the resultant inhomogeneous lines had been shifted to a lower frequency (figure 9) and the line had been broadened. The area under the lines remains constant to within the limits of accuracy of our experiment.

(iii) Allowing the crystal to rise to a temperature of greater than 50 K and then recooling to 10 K or lower returned the line profile to its original shape and position.

Figure 7 shows that for each site there are two equivalent positions for the uranium ion, displaced either positively, U', or negatively, U", along the *c* axis from the substitutional site. In an ideal crystal the sites will be iso-energetic with a potential barrier between the two sites. In a real crystal the two sites are likely to be experiencing a different potential due to defects in the crystal structure which cause the inhomogeneity of the zero-phonon lines. The crystal will therefore have an ensemble of centres each having two alternative ground-state sites, U' and U", with varying gaps between their ground-state energies, schematically illustrated in figure 10. This situation and the ensuing proposed mechanism for hole-burning is very similar to the two-level system
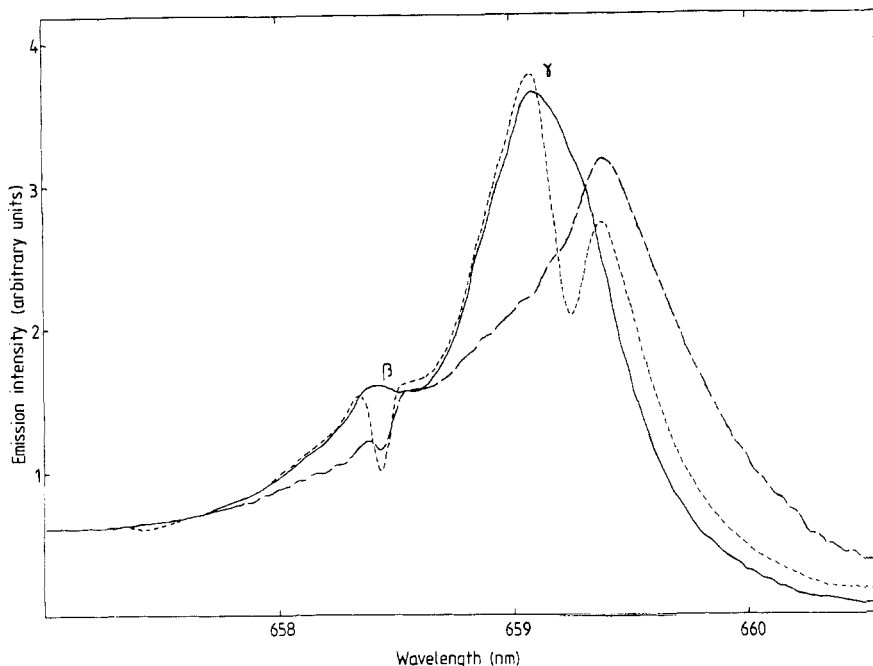
Figure 9. Excitation of the β- and γ-lines in the concentrated crystal at 10 K recorded in σ-polarisation. The full curve is that obtained upon cooling the crystal from room temperature. A second trace (the broken curve) gives the spectrum after hole-burning at a frequency on the low-energy side of the γ-line. As well as the holes at the burn frequency and the associated one in the β-line, note that the anti-holes are predominantly at lower energy. This gives an apparent broadening of the zero-phonon line towards lower energy. The chain curve gives the spectrum after pumping the α zero-phonon line. This causes removal of holes and a displacement of both β and γ zero-phonon lines to lower energy.
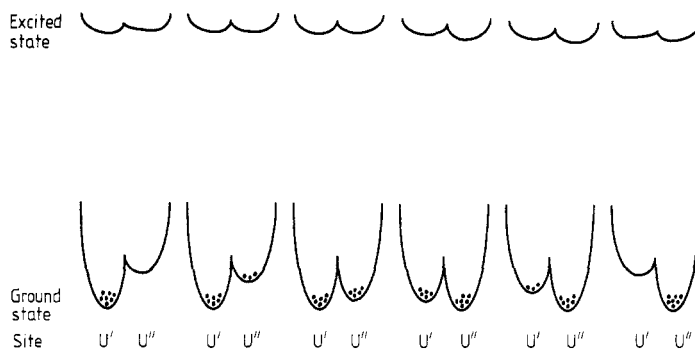

Figure 10. A schematic illustration of potential energy wells for the position of the substitutional uranium ions. At each site there are two sites, U' and U", as indicated in figure 6. With random internal lattice strain the relative depth of the two wells can be varied. The population within the wells attained with slow cooling is indicated by the small full circles.

Table 2. Maximum attained hole depths for strontium tungstate.

Doping concentration Laser resolution Zero-phonon line	200 ppm		500 ppm	
	1 MHz	30 GHz	1 MHz	30 GHz
α	—	20%	—	<5%
β	>90%	>90%	>90%	70%
γ	>90%	>90%	>90%	70%

that has been well utilised to explain hole-burning in glassy systems (Hayes *et al* 1988). The major difference being that the two-level description of glasses as first proposed by Anderson *et al* (1972) and Phillips (1972) is an approximation for the many degrees of freedom present in a glass whereas here there are strictly only two ground states possible for each substitutional site. A better analogy might be that of ReO_4 molecules in alkali halides where the ion can substitute in two different orientations (Sievers 1985).

It is proposed that hole-burning occurs when the centre is excited from the ground state to the excited state and relaxes back to the electronic ground state, but the location is changed during the process. Once in the new site there is insufficient thermal energy for the ion to return to the original site. The hole is created because the frequency of the electronic transition to the excited state will now be different. All transitions at the laser (burn) frequency could become completely removed by this pumping cycle resulting in very deep holes. This is the case for the β- and γ-lines into which holes approaching 100% deep can be burnt by irradiating with 100 mW for 30s using the high-resolution laser (table 2). However when the low-resolution laser was used a hole of only 70% depth could be burnt in the β- and γ-lines and is attributed to a sizable fraction of the centres having their alternative resonant frequencies within the 30 GHz linewidth of the laser. Similarly, the α-line shows only shallow hole-burning (table 2) because there will only be a small number of the centres for which the shift in frequency is larger than the homogeneous linewidth.

The changes in the zero-phonon lineshape which occur upon optical pumping or thermal cycling, (ii) and (iii), can also be understood if the frequency of the anti-hole is considered in more detail. There is a distribution in the energies of the U' and U" sites and when the crystal is first cooled the lower potential energy position will be favoured. Holes burnt at 5 K were cycled to 30 K for several minutes without a significant loss of hole depth suggesting that little orientation takes place below 30 K thus preventing an exact Maxwell–Boltzmann distribution for lower temperatures. If then there is some correlation between the ground-state energy and the corresponding absorption frequency, as can occur when the strain has little effect on the excited-state energies (figure 10), the observed zero-phonon line will have a dominant contribution from higher frequencies. Slow cooling therefore will give a zero-phonon line biased to higher energies.

A different distribution of centres will be attained with optical pumping and this will result in a different zero-phonon life profile. When all the centres are excited with equal probability by pumping evenly over the width of the zero-phonon line or pumping within the homogeneously broadened vibronic band the population of the various potential wells will be evenly distributed. The associated zero-phonon line will correspondingly have a more even contribution from all wells and hence be at lower frequency than that
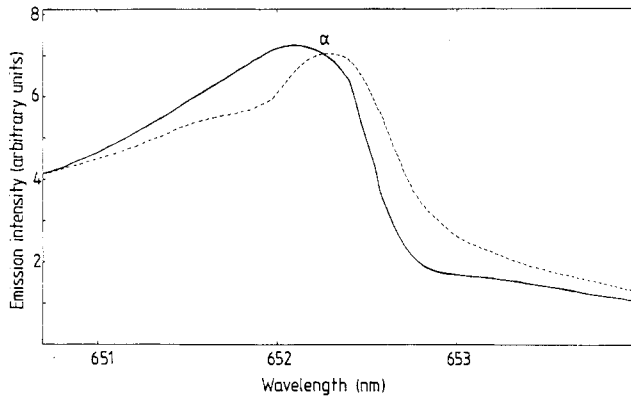
Figure 11. The α zero-phonon line in the concentrated $SrWO_4$: U sample at 10 K measured in σ-polarisation. The full curve gives the spectra obtained upon slow cooling whereas the broken curve gives that attained after hole-burning at 652.0 nm using 180 mW for 15 min.

attained by slow cooling. If, therefore, a sample for which a hole has been burned in the γ or β zero-phonon line is subsequently irradiated at the frequency of the α zero-phonon line, with its much larger homogeneous width (as described in (i)) a wide range of centres will be excited. This irradiation will result in a zero-phonon lineshape close to that described for broad-band pumping. This has the effect of eliminating the holes and displacing the line further to lower energies (figure 9).

The effect of narrow-band pumping or hole-burning is to depopulate centres with absorption at the laser frequency regardless as to whether the absorption is associated with a high- or low-energy potential well. The absorption is not lost but merely shifted to the frequency of the complementary uranium location. Starting with a sample which has been slowly cooled where the uranium ions are predominantly in their low-energy sites, hole-burning will have the effect of displacing them to their high-energy sites. The associated new absorption will in general be displaced to lower energy. This is seen in figure 9 where hole-burning within the γ zero-phonon line decreases absorption at the burn frequency but increases the absorption at lower energy, and longer wavelength.

Hole-burning in the α zero-phonon line itself is analogous but less obvious. Figure 11 shows the profile of the concentrated $SrWO_4$ sample before and after burning a hole for 15 min with a 200 mW beam. A shallow broad hole is just visible but in addition the overall line profile has been shifted to lower energies. Broad-band pumping or thermal cycling after hole-burning will erase the hole and restore the zero-phonon lineshape as discussed in the previous paragraph.

In all of the above cases the overall absorption or excitation intensities integrated over the zero-phonon line remain constant. This is the important characteristic to establish the hole-burning mechanism as photophysical rather than photochemical.

3.5. The hole-burning efficiency

Much of the interest in spectral hole-burning concerns the search for a material suitable for optical data storage (Castro *et al* 1978) in which both frequency and spatial domains are used for storing logical 'ones' and 'zeros' as 'holes' or 'no holes'. An important parameter for deciding what sort of materials may be suitable for optical data storage is hole-burning efficiency. This is defined as being the probability that a photo-induced

change will occur when a centre absorbs a photon. A high hole-burning efficiency would result in a reduced 'write' time but would increase the erasure of data during reading.

In terms of $(\mathrm{d}T(t)/\mathrm{d}t)_{t=0}$, the initial hole-burning rate in terms of transmission, T_0, the initial sample transmission, I, the laser intensity, h, Planck's constant $(6.6 \times 10^{-34}$ J s$)$, ν, the laser frequency, R, the total reflection loss, and s, the absorption cross section, it can be shown (Moerner *et al* 1984) that the hole-burning efficiency, η, is given by

$$\eta = \frac{(\mathrm{d}T(t)/\mathrm{d}t)_{t=0}}{sT_0(I/h\nu)(1 - T_0 - R)}.$$

$(\mathrm{d}T(t)/\mathrm{d}t)_{t=0}$ was found to be 0.065 s^{-1} when burning in the γ zero-phonon line of SrWO$_4$:U with $T_0 = 0.96$, using a laser beam with $I = 10^5$ W m^{-2} and $\nu = 4.5 \times 10^{14}$ Hz. The value of R is taken to be negligible.

The absorption cross section, s, is equal to the ratio of the absorption coefficient of the centre at the laser frequency to the density of centres within one homogeneous linewidth of the laser frequency, N_ν. For high initial sample transmission, the laser frequency absorption coefficient is simply the ratio of the crystal absorption to crystal length, L, that is, $(1 - T_0)/L$. For a hole limited by laser linewidth, $\Delta\nu_{\mathrm{laser}}$, the proportion of centres within one homogeneous linewidth of the laser is $\Delta\nu_{\mathrm{laser}}/\Delta\nu_{\mathrm{inhom}}$ (for holes burnt near to the line centre) where $\Delta\nu_{\mathrm{inhom}}$ is the inhomogeneous linewidth of the zero-phonon line. If P is the proportion of tungsten ions replaced by uranium ions, ρ is the density of SrWO$_4$ (6200 kg m^{-3}), N_A is Avogadro's number (6×10^{23}) and M is the molecular mass of SrWO$_4$ (0.34 kg) then N_ν is given by

$$N_\nu = (\Delta\nu_{\mathrm{laser}}/\Delta\nu_{\mathrm{inhom}})P\rho N_A/M.$$

Substituting our data for a SrWO$_4$ crystal with $L = 2$ mm, $\Delta\nu_{\mathrm{inhom}} = 10^{11}$ Hz and $P = 2 \times 10^{-4}$ gives a hole-burning efficiency of the order of 10^{-4}. This hole-burning efficiency is thought to be too low to be of any technological interest (Moerner and Levenson 1985).

The low quantum efficiency provides evidence that the system also experiences a distortion in the excited state. This is concluded from the fact that for every ten thousand times the transition is excited the uranium ion, during its 20 μs lifetime in the excited state, can only tunnel once to its alternate site to produce an optical hole. Had there been no such barrier to reorientation the hole-burning efficiency would be 0.5 corresponding to relaxation to either equilibrium site with equal probability. It is further possible that the reorientation does not occur in the excited state at all but rather in the ground state during the relaxation cycle. For example there is radiative decay to vibrational levels up to 800 cm^{-1} above the ground state and in these states there will be enough energy to cross the potential barrier. Evidence for this is the fact that when the sample is heated to 50 K, weakly populating such vibrational levels, spectral holes are eliminated.

4. Summary

Spectral holes have been burnt in SrWO$_4$:U and BaWO$_4$:U which has allowed us to use techniques of high-resolution spectroscopy to determine the site symmetry of the centre in SrWO$_4$:U. Quadratic Zeeman shifts of the narrow spectral holes have shown

that the substitution of U^{6+} ions is distorted in one of two crystallographically equivalent directions along the c axis. This reduces the centre symmetry from S_4 (tetragonal) to C_2 (monoclinic). The α, β and γ zero-phonon lines are assigned to states that transform as Γ_2, Γ_1 and Γ_2 irreducible representations respectively and a further Γ_1 state lies at higher energies.

The hole-burning mechanism has been shown to be photophysical, arising from the reorientation of the uranium at the substitutional site. The hole-burning efficiency of 10^{-4} is too low for these materials to be of practical use for digital information storage.

References

Anderson P W, Halperin B I and Varma C M 1972 *Phil. Mag.* **25** 1–9
Castro G, Haarer D, Macfarlane R M and Trommsdorff H P 1978 *Frequency selective optical data storage system; US Patent Specification* 4101976
Denning R G, Snellgrove T R and Woodwark D R 1976 *Mol. Phys.* **32** 419–42
—— 1979 *Mol. Phys.* **37** 1109–43
Hay P J 1983 *J. Chem. Phys.* **79** 5469–82
Hayes J M, Jankawiak R and Small G J 1988 *Persistent Spectral Holeburning: Science and Applications* ed. W E Moerner (Berlin: Springer)
International Tables for X-ray Crystallography 1969 vol 1 (Birmingham: Kynoch)
Jessop P E, Muramoto T and Szabo A 1980 *Phys. Rev.* B **21** 926–36
Macfarlane R M and Lenth W 1986 *Tunable Solid State Lasers II* ed. A M Budgor, L Esterowitz and L G De Shazer (Berlin: Springer) pp 14–8
Macfarlane R M and Shelby R M 1987 *Spectroscopy of Solids Containing Rare Earth Ions* ed. A A Kaplyanskii and R M Macfarlane (Amsterdam: North-Holland) pp 51–185
Macfarlane R M and Vial J-C 1986 *Phys. Rev.* B **34** 1–4
Moerner W E, Gehrtz M and Huston A L 1984 *J. Phys. Chem.* **88** 6459–60
Moerner W E and Levenson M D 1985 *J. Opt. Soc. Am.* B **2** 915–24
Morozov A M, Morozova L G and Feofilov P P 1972 *Opt. Spectrosc.* **32** 50–4
Phillips W A 1972 *J. Low Temp. Phys.* **7** 351–60
Runciman W A, Srinivasan B and Saebo S 1986 *Aust. J. Phys.* **39** 555–64
Sievers A J 1985 *Cryst. Latt. Defects Amorph. Mater.* **12** 441–57
't Lam R U E and Blasse G 1980 *J. Chem. Phys.* **72** 1803–8